Reconfiguration of Active Distribution Networks Equipped with Soft Open Points Considering Protection Constraints

Ali Azizi, Behrooz Vahidi, and Amin Foroughi Nematollahi

Abstract—**The purpose of active distribution networks (ADNs) is to provide effective control approaches for enhancing the operation of distribution networks (DNs) and greater accommodation of distributed generation (DG) sources. With the integration of DG sources into DNs, several operational problems have drawn attention such as overvoltage and power flow alteration issues. These problems can be dealt with by utilizing distribution network reconfiguration (DNR) and soft open points (SOPs). An SOP is a power electronic device capable of accurately controlling active and reactive power flows. Another significant aspect often overlooked is the coordination of protection devices needed to keep the network safe from damage. When implementing DNR and SOPs in real DNs, protection constraints must be considered. This paper presents an ADN reconfiguration approach that includes DG sources, SOPs, and protection devices. This approach selects the ideal configuration, DG output, and SOP placement and control by employing particle swarm optimization (PSO) to minimize power loss while ensuring the correct operation of protection devices under normal and fault conditions. The proposed approach explicitly formulates constraints on network operation, protection coordination, DG size, and SOP size. Finally, the proposed approach is evaluated using the standard IEEE 33-bus and IEEE 69-bus networks to demonstrate the validity.**

Index Terms—**Distributed generation, network reconfiguration, protection system, soft open point.**

I. Introduction

THE efficiency and reliability of distribution networks (DNs) have been decreasing owing to the constant increase in electricity consumption. The performance of a DN becomes inefficient owing to the decrease in voltage and increase in power losses [1]. Hence, modifications of the design and operating environment of power systems have necessitated the consideration of active distribution networks (ADNs) [2]. The power loss is typically reduced via several approaches: using power quality devices, applying demand response programs, reducing the network imbalance, improving the power factor [3], raising networks to higher voltage levels, using distributed generation (DG) units [4], and using the power electronic devices [5] placed in DNs [6].

DG sources are grid-connected or standalone electric generation units located within DNs. The integration of DG sources into a DN leads to an improvement in the voltage profile, reliability amendments (such as service restoration and uninterrupted power supply), and enhanced efficiency [7]. At the same time, a DN faces additional issues because of high DG penetration. The most prominent issues include the alteration of the current flow (which may surpass thermal loading in the event of low loading or high generation), voltage violations, and protection hazards, particularly the lack of coordination between protection devices [8], [9].

In DNs, there are typically a few normally open points connecting nearby feeders. These normally open points (tie switches) can be closed (while opening other switches) to reshape the network topology [10]. The process of altering the configuration of networks to accomplish certain goals by changing the states of sectionalized (closed) and tie (open) switches is referred to as distribution network reconfiguration (DNR). DNR can be used to mitigate power losses as a fairly simple and inexpensive solution to improve the overall voltage profile, balance the loads between feeders, and reduce the need for network reinforcement while considering the impact and increased penetration of DG units [11].

Another solution to complementing DNR and DG sources is to employ power electronic devices. By placing these devices—specifically, soft open points (SOPs)—instead of normally open points in a DN, the network capacity can be more effectively used [12]. An SOP is defined as two or more voltage-source converters (VSCs) connected via a common DC link. These devices provide reactive power and transfer active power between the AC terminals [9], efficiently compensating for DNs' lack of power control capability. Rather than just opening and closing the switches, an SOP may help balance the load flow and improve the network voltage profile [13]. The impacts of DG sources, DNR, and SOPs significantly affect the power flow in ADNs and therefore pose challenges to protection systems. As a result, the existing protection systems of ADNs need to be analyzed to guarantee that the protection devices accurately function in the case of faults.

Manuscript received: July 18, 2022; revised: October 6, 2022; accepted: December 9, 2022. Date of CrossCheck: December 9, 2022. Date of online publication: January 27, 2023.

A. Azizi, B. Vahidi (corresponding author), and A. F. Nematollahi are with the Department of Electrical Engineering of the Amirkabir University of Technology, Tehran, Iran (e-mail: aliazizi74@aut. ac. ir; vahidi@aut. ac. ir; amin. foroughi@aut.ac.ir).

DOI: 10.35833/MPCE.2022.000425

Several protection methodologies have been developed to limit the high DG penetration effects in DNs, utilizing both traditional and modified protection systems [14], [15]. However, only a few solutions incorporating DNR have been developed [16]. Reference [17] demonstrates the design procedure for a protection system for a reconfigurable IEEE 33-bus network considering all permissible configurations. The restrictions imposed by the coordination of the protection system and their requirements for the switching of relays are studied. Reference [18] presents detailed constraints as penalty functions on the DNR technique with an objective function for the power losses and a voltage profile that concentrates on the coordination of the existing protection devices. The studies on DNR with protection analyses in [17] and [18] do not address the addition of DG sources or SOPs.

Reference [19] develops an optimal DG placement approach that maximizes the penetration level of DG sources in DNs without modifying the original relay protection schemes using an impact analysis of the number of DG sources, their positions, and the capacities of the short-circuit current. Reference [20] presents further advanced research including a network-zoning-based (islanded) protection and reconfiguration technique for DNs with DG. However, neither [19] nor [20] focuses on evaluating the power losses or voltage profile concerns. The ideal switching configuration has been investigated in [21] that offers the lowest active power losses and a better voltage profile during which the protection devices effectively function under normal and faulty conditions. Reference [22] discusses a reconfiguration approach that considers protection limitations in the presence of DG units with an objective function for the power loss. A novel scenario-based algorithm also examines the uncertainties in the loads and power production of DG units.

In [23], a holistic framework for mitigating the DG of diverse effects using SOPs has been proposed, allowing the most convenient system configuration and better energy utilization for ADNs. A multi-objective optimization framework for improving the operation of a DN considering various penetration levels of DG sources is investigated in [24]. The study concludes that SOPs effectively improve the network performance in terms of power loss reduction, load balancing, and voltage profile enhancement. However, the effects of SOPs on the protection of ADNs during DNR have not been considered in any of the aforementioned papers.

To the best of the authors' knowledge, extremely limited research has been conducted on DNR with SOP integration while maintaining protection coordination to reduce power loss thus far. Rather, during the planning stages, DNR research has only focused on issues such as power losses, the voltage profile of each bus, and the size and placement of DG sources, whereas the impacts of protection systems are disregarded in the operational stage. Another noteworthy feature of the research is that it makes use of the existing protection systems (when determining the optimal network configuration and/or installing SOPs or DG sources in the DN) rather than investing in costly new protection equipment. This approach is consistent with the currently implemented real-world approach because changing the initial protective mechanism of a DN is both costly and technically complex. Furthermore, although the installation of SOPs in DNs does not require network reconfiguration, the current distributed protection system must be changed to allow these devices to cooperate with the SOPs. The simultaneous operation of the protection system with the SOPs has not been explicitly discussed before, and it is considered in this paper.

The remainder of this paper is organized as follows. In Section II, the model for SOPs is presented. Section III presents the mathematical problem formulation and constraints. and the methodology is presented in Section IV. Simulation results for IEEE 33-bus and IEEE 69-bus networks are discussed in Sections V and VI, respectively. Lastly, in Section VII, the conclusions are presented.

II. Model for SOPs

An SOP is a multipurpose power electronic device that replaces the tie-line switches between two buses in DNs as an active/reactive power flow control device. This paper utilizes a back-to-back VSC consisting of two insulated gate bipolar transistor (IGBT) based VSCs. On their DC sides, the VSCs are paired in series and share a common capacitor. Both VSCs generate voltage waveforms with the desired amplitude and phase angle on their own. This back-to-back form enables complete active power control through the DC link and an independent reactive power supply or intake at both VSC terminals [25]. A back-to-back VSC-based SOP in the *P*-*Q* control mode for one of the VSCs and in the V_{DC}-*Q* mode for the other VSC in the steady state allows for smooth control of the voltage and active/reactive power flow. A generic power injection model is considered for the normal operation of an SOP, as shown in Fig. 1.

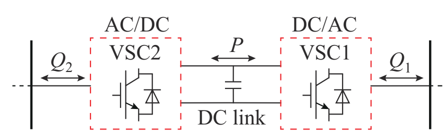

Fig. 1. Power injection model for an SOP.

The terminal power injections of SOP are considered in this model, allowing the SOP to be directly coalesced into current power flow analysis. In this model, the SOP is regarded as a line between two feeders that can manage the magnitude and direction of the active power flow and control the reactive power but with different magnitudes and directions (Q_1^K, Q_2^K) with respect to the capacity and limits of the converters ($Q_{\min}^K$, $Q_{\max}^K$). As a result, we can obtain:

$$P_1^K + P_2^K + P_{loss,SOP}^K = 0 \quad K \in N_{SOP} \tag{1}$$

$$Q_{1\min}^K \le Q_1^K \le Q_{1\max}^K \quad K \in N_{SOP} \tag{2}$$

$$Q_{2\min}^K \le Q_2^K \le Q_{2\max}^K \quad K \in N_{SOP} \tag{3}$$

where P_1^K and P_2^K are the active power with different magnitudes and directions; $P_{loss,SOP}^K$ is the active power loss of each converter in the K^{th} SOP; and N_{SOP} is the number of SOPs. Hence, the total power loss of the SOPs $P_{losses,SOP}$ is formulated as follows.

$$P_{losses,SOP}=\sum_{K=1}^{N_{SOP}}P_{loss,SOP}^{K} \tag{4}$$

$$P_{loss,SOP}^{K}=A_{loss,SOP}\sqrt{(P^{K})^2+(Q^{K})^2} \quad \forall K\in N_{SOP} \tag{5}$$

where $A_{loss,SOP}$ is the loss coefficient of VSCs, which represents the internal power loss of individual components for SOP. The VSCs connected to the feeders restrict the K^{th} SOP to a particular capacity S^K, necessitating both active and reactive power to meet it.

$$\sqrt{(P_1^K)^2+(Q_1^K)^2}\le S_1^K \quad K\in N_{SOP} \tag{6}$$

$$\sqrt{(P_2^K)^2+(Q_2^K)^2}\le S_2^K \quad K\in N_{SOP} \tag{7}$$

Under fault conditions, as suggested in [26], the dynamic performance of an SOP is determined using sequence networks such that DNs using SOPs may be analyzed using traditional fault analysis techniques. The symmetric voltage components obtained at the network connection point of SOP are used to create a fault index (FI). In less than two cycles of fault occurrence, the steady-state FI decreases significantly below the threshold value. Therefore, the SOP can be considered as an open switch. The IGBTs can be instantly turned off if the FI falls below a certain threshold. The study shows that calculating the FI takes almost no time. Compared with the current-based detection approach, which relies on a relay and an isolator, the proposed approach is substantially faster to implement. This approach demonstrates the ability of SOP to identify faults efficiently and quickly.

III. Mathematical Problem Formulation and Constraints

A. Objective Function

The purpose of this paper is to determine the best configuration, DG size, and SOP location and control while guaranteeing that the existing protection devices continue to function properly in a coordinated manner. The objective function of this optimization process OF is defined to minimize the power loss of each line and the power losses of the connected VSCs.

$$OF=\min(P_{losses}+P_{losses,SOP}) \tag{8}$$

$$P_{losses}=\sum_{n=1}^{M}Real(Z_n|I_n|^2) \tag{9}$$

where P_{losses} is the total active power loss in the DN; M is the number of branches; Z_n is the impedance of line n; and I_n is the current flowing through line n. The control variables include the statuses of the switches (both tie and sectionalized) in the lines, the SOP location and control (the active power flow value and direction and the reactive power flow value injected or absorbed at both terminals), and the active power output of DG units into the DN.

B. DNR Constraints

After the DNR procedure, the network topology must be radial. This implies that all buses must be linked to the main substation and that there must be no network loops. Another constraint is the magnitudes of the voltages of the buses, which are usually set to be ±10% of the rated voltages. Because of security and thermal concerns, I_n should not surpass the limit of the branch current.

$$V_{\min}\le V_{bus}\le V_{\max} \tag{10}$$

$$I_n\le I_n^{\max} \tag{11}$$

where $V_{\min}$, V_{bus}, and $V_{\max}$ are the minimum voltage, bus voltage, and maximm voltage, respectively; and $I_n^{\max}$ is the maximum current of line n.

C. DG Constraints

To function properly during the DNR process, the operation and size of DG sources must be regulated by the following constraints.

1) DG Capacity

The maximum and minimum capacities of the DG sources, i.e., $P_{DG}^{\max}$ and $P_{DG}^{\min}$, respectively, restrict the DG size P_{DG}:

$$P_{DG}^{\min}\le P_{DG}\le P_{DG}^{\max} \tag{12}$$

2) Power Injection

Equation (13) defines a constraint that prevents the current flowing from DG sources to the grid, possibly disrupting the grid protection mechanism.

$$\sum_{i=1}^{N_{DG}}P_{DG,i}<\sum_{n=1}^{N_{bus}}P_{load,n}+P_{losses} \tag{13}$$

where $P_{load,n}$ is the load at bus n; N_{DG} is the number of DG sources; N_{bus} is the number of buses; and $P_{DG,i}$ is the size of the i^{th} DG.

3) Power Balance

Equation (14) guarantees that the power consumed by the load, including the losses of the devices and lines, equals the total power produced by the main substation $P_{substation}$ and the DG sources.

$$\sum_{i=1}^{N_{DG}}P_{DG,i}+P_{substation}=\sum_{n=1}^{N_{bus}}P_{load,n}+P_{losses} \tag{14}$$

D. Protection Constraints

The existence of DG sources and SOPs and the implementation of DNR cause the line current to change. The DG sources and SOPs in the DN help notably decrease power losses and enhance the voltage profile of each bus, but they could have adverse effects on the protection and coordination of the DN if no protection constraints are considered. If the new line current following a new configuration or the installation of SOPs surpasses the ratings of the protection devices installed in the network, they will trip and cut the supply of the protection zone. Miscoordination of the primary protection and backup protection device can also be a repercussion when the constraints of the protection are not considered with the DNR procedure.

To minimize erroneous tripping and protection blinding, the protection of the new configuration must be able to separate the faulty area. In practice, network operators prefer to avoid expensive expenditures by avoiding the modification of current protection measures [18]. Therefore, the following constraints must be applied to ensure that changes in the current flow do not cause protection devices to fail to operate accurately and unwanted power outages in the ADN.

1) Overload Factor Limit

Suppose that the branch current surpasses the pick-up current of the relay or recloser or the operating current of the fuse under normal operating conditions. To prevent the damage to equipment, the protection equipment must be able to isolate the overloaded region quickly. To consider overloaded conditions, the overload factor (OLF) is considered and formulated as:

$$I_n \cdot OLF < I_p \tag{15}$$

where I_p is the operational pick-up current of the protection device.

2) The Minimum Fault Current Sensitivity

To prevent the operation failure under fault conditions, the minimum fault current $I_{f,\min}$ must be greater than the rated I_p of the protection device. Owing to this constraint, the protection device can identify the problem and isolate the faulty area. The constraint avoids protection blindness, which would result in a portion of the DN being left uncovered and unprotected.

$$I_p < I_{f,\min} \tag{16}$$

E. Protection Coordination

The coordination among series-connected protection devices under fault conditions is necessary and has multiple criteria. It is essential to determine the main and backup functions of each protection device to avoid unnecessary outages in DNs. Furthermore, from the perspective of fault current alterations, the effects of DG sources and SOPs on the DN must be adequately considered. Four types of coordination among protection devices are examined: fuse-fuse, relay-fuse, relay-downstream, and relay-relay coordinations.

1) Fuse-fuse Coordination

The primary fuse must act first to isolate the problem before the backup fuse may operate in the concept of protection coordination. The clearing time of the main fuse must be less than 75% of the minimum melting time (MMT) of the backup fuse.

$$MCT_{F_m} \le 75\% \cdot MMT_{F_b} \tag{17}$$

where MCT_{F_m} is the maximum clearing time (MCT) of the main fuse; and MMT_{F_b} is the MMT of the backup fuse.

2) Relay-fuse Coordination

A coordination time interval (CTI) is considered between the trip time of the downstream protection (primary protection) and the relay as the backup. If the main protection device fails, the CTI guarantees that the backup device will act and eradicate the fault within the shortest possible period, ensuring the selectivity as:

$$t_{op} - t_{fuse} > CTI \tag{18}$$

where t_{fuse} is the trip time of the downstream protection device; and t_{op} is the relay operating time. The operational characteristic or time-current characteristic (TCC) of the relay may be mathematically defined using the following equation, per IEC and ANSI/IEEE standards:

$$t_{op} = \frac{TDS \cdot \beta}{PSM^{\alpha} - 1} + L \tag{19}$$

where β, α, and L are the constants established by the standards defining different types of inverse time relays. According to (20), the term PSM denotes the plug setting multiplier, which is the ratio of the fault current I_{fault} to the pick-up current of the relay $I_{pick\text{-}up}$.

$$PSM = \frac{I_{fault}}{I_{pick\text{-}up}} \tag{20}$$

3) Relay-downstream Coordination

The reclosers feature two trip modes: fast and delayed (slow) trip modes with varying speeds. The fast trip mode protects downstream fuses from temporary disturbances and faults. The delayed trip mode is configured as backup protection in the case where the fuses fail to operate. The coordination of the recloser setting is set to the initial network configuration, and the changes made by DNR may affect relay-downstream coordination. The following constraint must be used to guarantee recloser coordination with other protection devices in the optimization process to find the optimal configuration while the coordination constraint remains satisfied.

The coordination requirements of a downstream fuse and a recloser on the upstream side are as follows.

The MMT of the fuse must be at least k times longer than the time of fast operation t_{fast}.

$$\frac{MMT}{t_{fast}} > k \tag{21}$$

Furthermore, the slow mode of the closer, t_{slow}, must be larger than the MCT of main fuse with a predesignated CTI.

$$t_{slow} - MCT > CTI \tag{22}$$

4) Relay-relay Coordination

The basic guidelines for proper relay coordination can be summarized as follows.

Pair relays have the same operational characteristics in series with one another whenever it is possible. I_p needed to run the relay in front must always be equal to or less than the primary current required to operate the relay behind it. To ensure that the circuit breaker closest to the problem opens first, an adequate time interval is considered between the relays that control the circuit breakers in the DN. The CTI between each relay time setting must be sufficiently long to ensure that the upstream relays cannot operate before the circuit breaker closer to the fault location has tripped and cleared the fault [18], [21], [27].

$$t_{op,backup} - t_{op,main} > CTI \tag{23}$$

where $t_{op,backup}$ and $t_{op,main}$ are the operation time of the backup and main relays, respectively.

IV. Methodology

The purpose of the proposed approach is to obtain the optimal network configuration, SOP placement and performance, and DG output while maintaining protection constraints. In this paper, the DG sources are assumed to be privately owned; therefore, their positions have been specified and fixed. Additionally, if a fault occurs at the end of a radial line, the DG may become an island and must be removed from the network, as specified by the IEEE 1547 standard. A flowchart and process framework of the proposed approach is shown in Fig. 2.

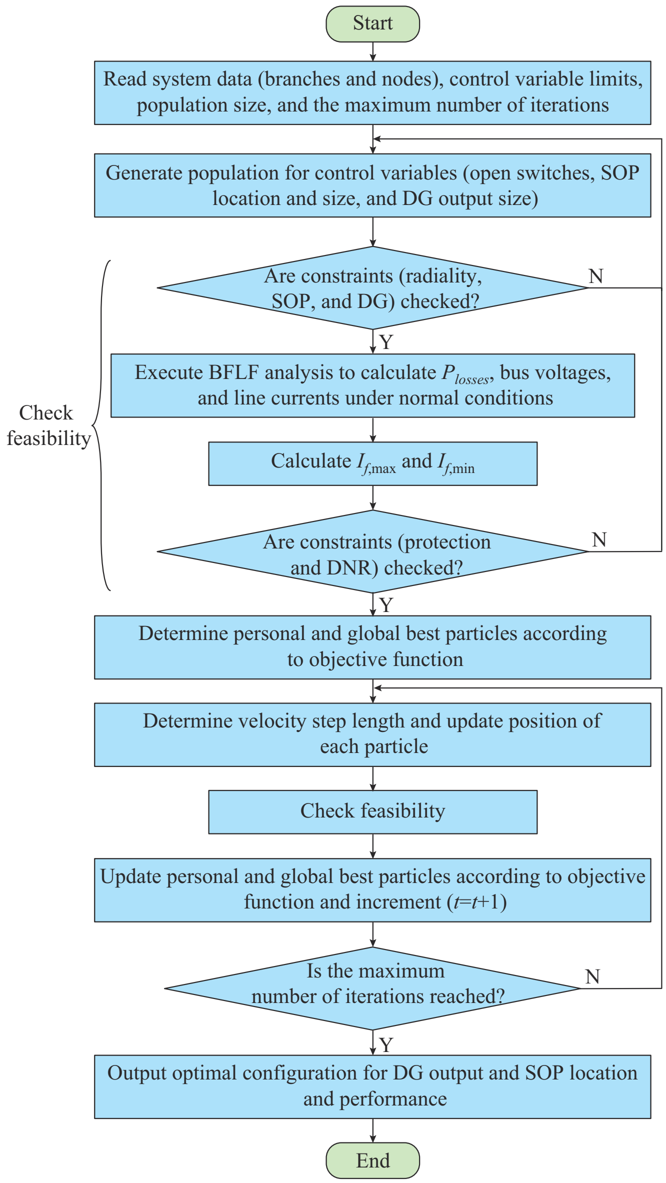

Fig. 2. Flowchart and process framework of proposed approach.

To establish the value of the objective function, the backward/forward sweep power flow (BFLF) technique [28] is used to evaluate the power losses, DG output, SOP performance, and line current, and to check the constraints. The radiality is confirmed by ensuring that the number of normally closed switches is one less than the number of buses and that all of the buses are connected. Subsequently, several combinations of open switches are investigated to discover and reach the minimum objective function by comparing the initial configuration and the new combination of switches in the network after DNR. In the optimization approach, the protection constraints are considered. To efficiently discover the optimal configuration, an optimization approach is necessary because the complexity of DNR increases with the penetration of DG sources and SOPs. This complexity creates a sizable search space with an optimal point within it. Therefore, the particle swarm optimization (PSO) is used in this paper. PSO is used to simultaneously optimize DNR, the DG output, and the SOP performance. When evaluating the objective function (after the generation of particles and during the process of updating their positions), only configurations that fulfill all of the stated constraints are examined. MATLAB platform has been used to code and execute the proposed approach.

V. Simulation Results for IEEE 33-bus Network

The proposed approach is validated with standard IEEE 33-bus and IEEE 69-bus networks. Figure 3 shows a single-line diagram of the IEEE 33-bus network (12.66 kV) with a total load of 3.715 MW and 2.3 Mvar, and the apparent base power is assumed to be 100 MVA. The dotted red lines denote the switches that have been opened.

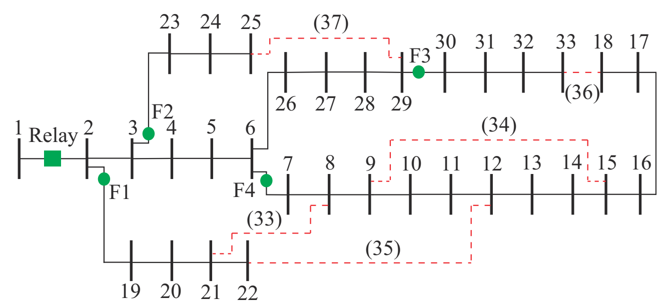

Fig. 3. Single-line diagram of IEEE 33-bus network.

Although any protection scheme can be used to assess the practicality of the protection constraints, the positions of the protection devices are depicted according to [18]. In Fig. 3, four fuses (F1-F4) are inserted at the beginning of the original configuration laterals as the main protection, and a relay is fitted immediately after the substation as the backup. The fuse size and the setting of the protection devices are assumed to be fixed. Owing to the proven performance and economic efficiency of the fuse, it is commonly employed in DNs. A primary advantage of the fuse over a circuit breaker is that it can stop very large short-circuit current in a shorter time period than that of a circuit breaker within its capacity. TCC fuse of S&C Electric Company (connection type: T) is employed in this paper [29]. A fixed CTI of 0.3 s and a time dial setting (TDS) of 1.65 s for the relays are assumed. An inverse definite minimum time relay ($\alpha=0.2$, $\beta=28.2$, $L=0.1217$) is selected because its operation characteristic is similar to the TCC of the selected fuses.

A three-phase-to-ground fault is considered for the maximum fault current in the short-circuit calculation at the location of each protection device. However, regarding the minimum fault current, a line-to-line fault is in the protected region of the bus, where there is smaller fault current. In fault situations, the load current is not considered. The load flow analysis, rating of protection device, and operation time in initial network are listed in Table I, where the open switches are 33, 34, 35, 36, and 37; the active power loss is 202.665 kW; and the minimum voltage of buses is 0.9131 p.u..

TABLE I
LOAD FLOW ANALYSIS, RATING OF PROTECTION DEVICE, AND OPERATION TIME IN INITIAL NETWORK

Protection device	Current setting (A)	Load current (A)	The maximum short-circuit current (A)	MCT (s)	t_{op}
Relay	316	210.35	5200		
F1	30	18.10	4870	0.0168	0.317
F2	80	48.49	3619	0.0522	0.474
F3	80	50.58	1081	0.4457	4.095
F4	100	58.39	1914	0.2411	1.390

Five case studies are conducted using the IEEE 33-bus network. Cases 1 and 2 only incorporate DNR and are evaluated without SOP and DG integrations, whereas cases 3 and 4 are evaluated with SOP integration. Case 5 is tested with the simultaneous integration of SOPs and DG sources. Protection constraints are used in cases 2, 4, and 5, whereas they are not considered in cases 1 and 3.

A. Case 1: Optimal Configuration Without DG, SOP, and Protection Constraints

Case 1 studies the implementation of DNR without protection constraints using PSO. The open switch (7, 9, 14, 32, 37) combinations, active power loss (139.55 kW), and the minimum voltage (0.9375 p.u.) of the buses are listed in Table II. Theoretically, the optimal global solution obtained using PSO indicates that the switches 7, 9, 14, 32, and 37 should be opened. In comparison to the initial configuration, DNR uses PSO to decrease the active power losses by 31.1% and increase the minimum voltage by 2.67%. To analyze the protection device conditions for case 1, Table II presents the load current and fault current flowing through the protection devices. F2, F3, and F4 perform normally under the assumed load and 25% overload conditions. As can be observed, even under normal loading conditions, F1 is overloaded because the load current passing through it will cause the fuse link to melt and unnecessarily break the circuit. These findings demonstrate the need to address the protection constraints during DNR to avoid network protection failure.

TABLE II
LOAD FLOW, LOAD CURRENT AND FAULT CURRENT, AND FUSE STATUS FOR CASE 1

Protection device	Load current (A)	25% overload (A)	The maximum fault current (A)	The minimum fault current (A)	Status
F1 (30 A)	67.77	84.72	4861	466.73	Open
F2 (80 A)	48.28	60.35	3619	1552.00	Closed
F3 (80 A)	46.18	57.72	1078	800.00	Closed
F4 (100 A)	10.55	13.19	1907	1714.00	Closed

B. Case 2: Optimal Configuration Without DG Sources and SOPs Considering Protection Constraints

The protection constraints are taken into account during optimization in case 2, and the results are summarized in Table III, where the optimization approach is PSO; the open switches are 11, 13, 32, 33, and 37; the active power loss is 181.1 kW; and the minimum voltage of buses is 0.9222 p.u.. The protection constraints eliminate all configurations that violate the operation requirements of the protection devices. It is observed that the active power losses of the network have increased in comparison with those for case 1, as anticipated, because additional constraints have been incorporated into the optimization problem. Nonetheless, the active power loss is less than the noted active power loss in the initial configuration. Table III also confirms the proper functioning of the protection system given that, under fault conditions, all of the fuses will melt and break the circuit as the minimum fault current are greater than the ratings of the fuses.

TABLE III
LOAD FLOW, LOAD AND FAULT CURRENTS, AND FUSE STATUS FOR CASE 2

Protection device	Load current (A)	25% overload (A)	The maximum fault current (A)	The minimum fault current (A)	Status
F1 (30 A)	23.52	29.17	4861	736	Closed
F2 (80 A)	48.45	60.56	3619	1552	Closed
F3 (80 A)	46.96	58.69	1078	800	Closed
F4 (100 A)	54.68	68.34	1907	535	Closed

C. Case 3: Optimal Configuration and SOP Performance with no Protection Constraints

Case 3 investigates the performance of the IEEE 33-bus network when implementing an SOP combined with DNR. Owing to its high cost, one SOP is considered in this paper and is installed in place of one of the tie-line switches. The addition of the SOP adds three additional control variables (P, Q_1, and Q_2) to the optimization problem. Each VSC in the SOP has the maximum capacity of 1 MVA. As mentioned in Section II, the SOP will trip almost instantly under fault conditions, which is why it is considered as an open switch in short-circuit calculations. Table IV presents the results for case 3 using PSO. From the simulation results, it is clear that the integration of the SOP into the network is beneficial, and the active power loss is considerably reduced compared with those for cases 1 and 2.

TABLE IV
RESULTS FOR CASE 3 USING PSO

Open switch	P_{loss} (kW)	The minimum voltage (p.u.)	SOP performance
7, 9, 14, 36, SOP at 37	95.7	0.9545	$P=0.3310$ MW, $Q_1=0.425$ Mvar, $Q_2=0.943$ Mvar

The results in Table V demonstrate that a protection device is overloaded and will melt and break the circuit in this configuration, even though the SOP has reduced the power loss. F1 is overloaded under both normal and overloaded conditions. Hence, the resulting structure and SOP performance are not feasible in the real world because they impede the proper functioning of the protection devices.

TABLE V
CURRENT PASSING THROUGH FUSES AND FUSE STATUS IN CASE 3

Protection device	Load current (A)	25% overload (A)	Status
F1 (30 A)	64.14	80.18	Open
F2 (80 A)	60.36	75.46	Closed
F3 (80 A)	48.10	60.13	Closed
F4 (100 A)	10.42	13.02	Closed

D. Case 4: Optimal Configuration and SOP Performance with Protection Constraints

In case 4, the optimization procedure is performed in the same way as shown in case 3 with one distinction: protection constraints are considered, and all instances in which the safety restrictions are not retained will be removed. The results show that, for practical applications, the optimization with the protection constraints is preferable, as shown by the results in Table VI, despite more power loss P_{loss} in case 4 compared with that in case 3. Under normal load and 25% overload conditions, the results in Table VII demonstrate that all security and protection requirements are met, preventing the damage to equipment or power outages in faultless areas.

TABLE VI
RESULTS FOR CASE 4 USING PSO

Open switch	P_{loss} (kW)	The minimum voltage (p.u.)	SOP performance
10, 12, 17, 33, SOP at 37	116.7	0.947	$P=0.401$ MW, $Q_1=0.486$ Mvar, $Q_2=0.915$ Mvar

TABLE VII
LOAD FLOW, FAULT CURRENTS AND OTHER PROTECTION PARAMETERS FOR CASE 4

Protection device	Load current (A)	25% overload (A)	The maximum fault current (A)	The minimum fault current (A)	MCT (s)	t_{relay} (s)
F1 (30 A)	23.70	29.7	4877	876	0.0168	0.317
F2 (80 A)	63.90	79.8	3630	1563	0.0522	0.474
F3 (80 A)	53.10	66.3	1080	706	0.4660	4.090
F4 (100 A)	46.26	57.8	1911	615	0.2460	1.390

E. Case 5: DNR, Optimal DG Size, and SOP Performance with Protection Constraints

Case 5 investigates the incorporation of DNR and an SOP into an ADN with protection constraints. Because electronically interfaced DG sources are restricted in their fault current contributions and are not subject to protection concerns, synchronous-machine-type DG sources are used in this paper. The DG sources are assumed to inject only active power. Three DG sources are considered, which are connected to buses 31, 32, and 33 [30]. The size and output of each DG source are determined after the optimization process to further reduce the total power loss. The DG sources have the minimum and maximum capacity sets of 0.1 MW and 1 MW, respectively. To prevent the current flowing from the network to the substation, the maximum DG penetration is restricted to 3 MW in the network (a total active load of 3.715 MW). The results in Table VIII show that the proposed approach, DNR, optimal DG output, and SOP control have significantly decreased the power loss compared with those for the previous cases.

TABLE VIII
RESULTS FOR CASE 5

Open switch	P_{loss} (kW)	The minimum voltage (p.u.)	DG output (MW)	SOP performance
10, 31, 33, 34, and SOP at 37	60.07	0.9746	0.760 (DG31), 0.557 (DG32), 0.182 (DG33)	$P=0.046$ MW, $Q_1=0.336$ Mvar, $Q_2=0.363$ Mvar

The fault-current level has increased owing to DG penetration. This increase is caused by the decreased fault impedances resulting from the parallel circuits created by the DG sources. The minimum fault current has also increased compared with those for previous cases, thus melting the fuse and isolating the faulty area in the network. The coordination between all protection devices still exists within the range of fault current. This demonstrates that the use of even a modest and low-rated SOP device instead of a tie switch substantially improves the overall network performance and outweighs its drawbacks.

The results in Table IX confirm that all of the protection constraints are satisfied. All fuses are the main protection devices in this configuration, as indicated in the optimal configuration in Fig. 4, and there is no backup fuse. The relay serves as the primary protection mechanism for certain buses and provides a backup to all fuses. The coordination between the fuses and relays is intact, and none of the fuses will trip under normal load or 25% overload conditions, surpassing the pick-up current of the fuses. Furthermore, the minimum fault current for all fuses is higher than the pick-up current; therefore, their sensitivity to faults is ensured.

The grid (bus 1), DG31, DG32, and DG33 all send fault current to the fault location. The proposed approach also eliminates the impact of sympathetic tripping. When a fault occurs at F4, a large fault current from the DG source positioned on bus 31 might cause F3 to operate incorrectly, particularly if the DG capacity is large. However, the incorrect operation is avoided in this case since the DG size is optimized, and F4 may act as the primary protection owing to the protection constraints with a sufficient CTI, isolating the faulty location before the other protection mechanisms kick in. Compared with the initial configuration, the proposed approach considering protection restrictions, appropriate DG size, and SOP control has considerably increased the minimum bus voltage. The introduction of DNR, the DG sources, and the SOPs has resulted in a noticeable improvement in the bus voltage. Table X compares all of the results of the IEEE 33-bus network with some equivalent cases in the literature.

TABLE IX
LOAD FLOW, FAULT CURRENT, FUSE STATUS AND OTHER PROTECTION PARAMETERS FOR CASE 6

Protection device	Load current (A)	25% overload (A)	Under the maximum fault			Under the minimum fault			Status
			The maximum fault current (A)	MCT (s)	t_{relay} (s)	The minimum fault current (A)	MCT (s)	t_{relay} (s)	
F1 (30 A)	23.79	29.74	5953	0.015	0.317	1571	0.120	8.64	Closed
F2 (80 A)	48.08	60.10	4597	0.038	0.492	1685	0.192	2.87	Closed
F3 (80 A)	36.80	46.00	2866	0.076	4.620	3063	0.512	5.41	Closed
F4 (100 A)	23.17	28.96	2991	0.108	1.532	1175	0.598	9.23	Closed

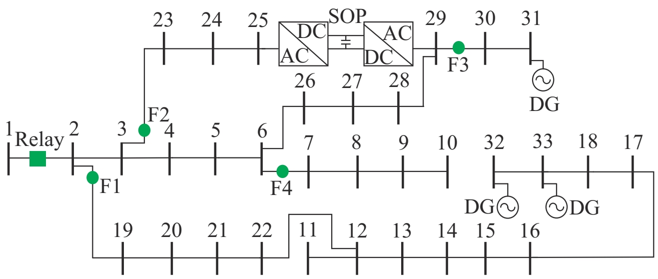

Fig. 4. Optimal configuration.

TABLE X
SUMMARY OF RESULTS FOR IEEE 33-BUS NETWORK COMPARED WITH THOSE IN [21] AND [12]

Type	Open switch	P_{loss} (kW)
Case 1	7, 9, 14, 32, 37	139.50
Case 2	11, 13, 32, 33, 37	181.10
Case 3	7, 9, 14, 36, SOP at 37	95.70
Case 4	10, 12, 17, 33, SOP at 37	116.70
Case 5	10, 31, 33, 34, SOP at 37	60.07
[21]	7, 9, 14, 32, 37	139.50
[21]	11, 13, 32, 33, 37	181.10
[12]	7, 9, 14, 36, SOP at 37	93.91

VI. SIMULATION RESULTS FOR IEEE 69-BUS NETWORK

The IEEE 69-bus network is investigated next, with 69 buses, 68 selectionizing switches, and five tie switches (69, 70, 71, 72, 73). The initial configuration is presented in Fig. 5. The simulation results show that the initial active power loss of the network is 224.56 kW and the minimum voltage is 0.9093 p.u. without any DG sources or SOPs.

Based on the initial configuration of the network, the positions of the protection devices are indicated in accordance with [18] and [21], despite the fact that any protection scheme can be used to evaluate the feasibility of the protection constraints. Compared with the previous network, the IEEE 69-bus network features an additional safety device: the recloser, which is placed at the outgoing feeder of bus 9. It is utilized to separate the protection zones of the main network branch. As a result, the coordination between the recloser and the downstream fuses (F6, F7, and F8), as well as the relay and downstream devices, will be the focus of the analysis of this IEEE 69-bus network.

If the main and backup fuses and the recloser cannot segregate a fault, the main relay serves as the subsequent protection layer. Therefore, the main relay is coordinated with the slow mode of the recloser. The TDS of the relay is 0.9 s, whereas the TDS of the recloser is 0.08 s and 1.7 s in the fast and slow modes, respectively. For a recloser in the fast mode, the coordination factor k should be 1.25. A CTI of 0.2 s is considered to coordinate fuses with the slow mode of the recloser.

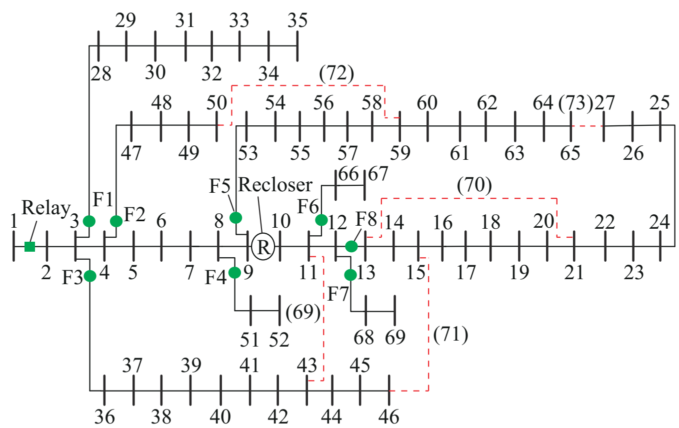

Fig. 5. Initial configuration of IEEE 69-bus network with five switches.

Moreover, the coordination of the relay with its downstream devices is achieved with the same CTI. With this setting, the protection devices in the initial configuration will function correctly and synchronously in the event of a system fault. Tables XI and XII list the coordination of the devices mentioned above, where I_L is the load current and $I_{f,\max}$ is the maximum fault current. With the integration of DG sources and SOPs into the IEEE 69-bus network, two case studies are conducted: DNR with no protection constraints (case 6) and DNR with protection constraints (case 7).

A. *Case 6: Optimal Configuration, DG Output, and SOP Performance with no Protection Constraints*

The results for case 6 are presented in Table XIII. The DG sources are connected to buses 60, 61, and 62 according to [30]. Except for F2 and F3, all fuses function properly under normal load and overload conditions, as shown in Table XIV. F3 is overloaded under normal loading conditions. Therefore, this configuration is not feasible under nonfault conditions. During a fault, the minimum fault current is sufficiently large to melt the appropriate fuse and prevent protection blinding. As can be observed, all fuses have a coordination factor greater than 1.25, which is required in the constraints; thus, the coordination is maintained in the fast mode. All downstream fuses meet the requirement that the CTI is greater than 0.2 s.

TABLE XI
COORDINATION OF RECLOSER WITH DOWNSTREAM FUSES IN INITIAL CONFIGURATION

Protection device	I_L (A)	25% overload (A)	$I_{f,\max}$ (A)	t_{fast} (s)	MMT (s)	k	t_{slow} (s)	MCT (s)	CTI
F6 (40 A)	2.08	2.60	2019	0.0122	0.026	2.17	0.259	0.046	0.213
F7 (30 A)	3.24	4.05	1674	0.0133	0.023	1.76	0.283	0.041	0.242
F8 (40 A)	20.41	25.51	1674	0.0133	0.038	2.89	0.283	0.061	0.220

TABLE XII
COORDINATION OF MAIN RELAY WITH DOWNSTREAM DEVICES IN INITIAL CONFIGURATION

Protection device	I_L (A)	25% overload (A)	$I_{f,\max}$ (A)	The maxmum operation time (s)	t_{relay} (s)	CTI
F1 (10 A)	5.13	6.41	4557	0.0138	0.2482	0.2344
F2 (80 A)	47.78	59.72	4553	0.0380	0.2485	0.2105
F3 (20 A)	10.32	12.90	4557	0.0149	0.2482	0.2344
F4 (6 A)	2.51	3.14	2909	0.0137	0.4527	0.4391
F5 (200 A)	105.23	131.54	2848	0.1532	0.4676	0.3144
Recloser	44.10	55.12	2848	0.2266	0.4676	0.2410

TABLE XIII
RESULTS FOR CASE 6

Open switch	P_{loss} (kW)	The minimum voltage (p.u.)	DG output (MW)	SOP performance
12, 13, 56, 69, SOP at 73	28.025	0.9784	0.298 (DG60), 1.200 (DG61), 0.202 (DG62)	$P=0.0034$ MW, $Q_1=0.097$ Mvar, $Q_2=0.49$ Mvar

TABLE XIV
PROTECTION PARAMETERS FOR CASE 6

Protection device	I_L (A)	25% overload (A)	$I_{f,\max}$ (A)	$I_{f,\min}$ (A)	k	CTI	Status
Relay (336 A)	144.14	180.17	6003				
F1 (10 A)	5.12	6.40	6002	986		0.230	Closed
F2 (80 A)	76.58	95.73	6000	249		0.216	Open
F3 (20 A)	27.70	34.63	6002	827		0.230	Open
F4 (6 A)	2.47	3.08	3377	2419		0.496	Closed
F5 (200 A)	3.09	3.87	3294	1938		0.411	Closed
Recloser (67 A)	23.19	28.98	3294	1519		0.302	Closed
F6 (40 A)	2.04	2.55	2229	1812	1.84	0.209	Closed
F7 (30 A)	3.16	3.96	1815	1315	1.56	0.235	Closed
F8 (40 A)	0	0	1815	827	2.56	0.218	Closed

B. Case 7: Optimal Configuration, DG Size, and SOP Performance with Protection Constraints

According to the optimal operation results of IEEE 69-bus network with SOPs and DG source in Table XV, the optimal configuration of IEEE 69-bus network is shown in Fig. 6. As indicated in Table XV, the suggested solution outperforms the initial configuration in terms of the reduction in the active power loss and the improvement in the minimum voltage. Nonetheless, when compared with case 6, which does not consider protection restrictions, the power loss expectedly increases by 20.45 kW.

TABLE XV
OPTIMAL OPERATION RESULTS OF IEEE 69-BUS NETWORK WITH SOPS AND DG SOURCE

Open switch	P_{loss} (kW)	The minimum voltage (p.u.)	DG output (MW)	SOP performance
13, 45, 69, 72, SOP at 73	48.48	0.9742	0.20 (DG60), 0.39 (DG61), 0.91 (DG62)	$P=0.0279$ MW, $Q_1=0.20$ Mvar, $Q_2=0.45$ Mvar

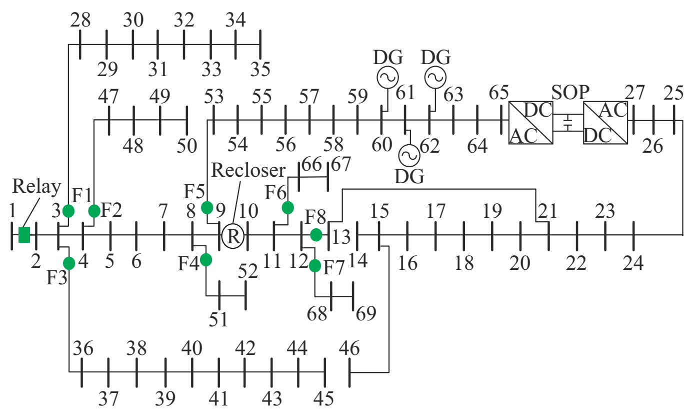

Fig. 6. Optimal configuration of IEEE 69-bus network.

Table XVI lists the load current flowing through each protection device. All protection devices are capable of detecting the minimum fault current in the protection zone while operating under normal load or 25% overload conditions. Table XVII shows that a coordination factor k of more than 1.25 has been achieved when the fast mode of the recloser is utilized. Therefore, the fast mode operation of the recloser is at least 25% faster than that of the MMT of the fuses, and quick coordination is ensured. In the process of slow-mode coordination, the recloser and downstream devices have worked together to meet the protection limitation requirement, with all CTIs above 0.2 s. It is concluded that the coordination of the recloser with downstream fuses is maintained in this scenario. The results in Table XVIII show that this configuration retains the coordination of relay and downstream device for more than 0.2 s.

TABLE XVI
LOAD CURRENT FLOWING THROUGH PROTECTION DEVICE

Protection device	Load current (A)	25% overload (A)	Status
Relay (336 A)	142.58	178.66	Closed
F1 (10 A)	5.12	6.40	Closed
F2 (80 A)	47.78	59.72	Closed
F3 (20 A)	8.16	10.20	Closed
F4 (6 A)	2.48	3.10	Closed
F5 (200 A)	38.02	47.73	Closed
Recloser (67 A)	39.78	49.88	Closed
F6 (40 A)	2.06	2.57	Closed
F7 (30 A)	3.20	4.01	Closed
F8 (40 A)	17.51	21.90	Closed

TABLE XVII
COORDINATION OF RECLOSER WITH DOWNSTREAM FUSE IN OPTIMAL CONFIGURATION

Protection device	$I_{f,\max}$ (A)	t_{fast} (s)	MMT (s)	k	t_{slow} (s)	MCT (s)	CTI (s)
F6 (40 A)	2642	0.0112	0.0157	1.4026	0.238	0.0330	0.205
F7 (30 A)	2068	0.0121	0.0153	1.2671	0.257	0.0319	0.225
F8 (40 A)	2068	0.0121	0.0254	2.1004	0.257	0.0448	0.212

TABLE XVIII
COORDINATION OF RELAY WITH DOWNSTREAM DEVICES IN OPTIMAL CONFIGURATION

Protection device	$I_{f,\max}$ (A)	The maximum operation time (s)	t_{relay} (s)	CTI
F1 (10 A)	5668	0.0137	0.2443	0.2307
F2 (80 A)	5665	0.0294	0.2445	0.2151
F3 (20 A)	5668	0.0143	0.2443	0.2301
F4 (6 A)	4276	0.0136	0.4227	0.4091
F5 (200 A)	4231	0.0767	0.4355	0.3588
Recloser (67 A)	4231	0.2189	0.4355	0.2166

VII. CONCLUSION

This paper presents a comprehensive framework using a new power electronic device, SOP, to enable the most efficient system configuration for improved ADN utilization, mitigate the adverse effects of DG, and consider the existing protection restrictions. In the presence of DG sources, DNR may result in wasteful tripping, longer downtime, and equipment failure for DNs. This paper aims to determine the network topology with the lowest power loss while maintaining the coordination of protection devices. Protection restrictions in terms of the operation and coordination of protection devices are clearly specified without the need to change the current protection systems.

The proposed approach is validated using IEEE 33-bus and IEEE 69-bus networks. Simulation results show that DNR has an obvious impact on the protection system. When DNR is used without considering the protection limits, configurations that are not viable for use in real-world DNs are developed. Despite a higher power loss than the ideal design without the protection limitation, the proposed approach provides the best configuration, DG sizes, and SOP placement and control, thereby allowing protection devices to function correctly. In addition to the advantages mentioned above, SOP control and presence assist in determining the optimal reconfiguration and controlling power flow over the network to achieve the desired results. Since DG penetration is increasing on a daily basis and upgrading old protection systems is both costly and complicated, the recommended solution could assist in achieving the best possible performance of DNs.

REFERENCES

[1] M. Siavash, C. Pfeifer, A. Rahiminejad *et al*., “Reconfiguration of smart distribution network in the presence of renewable DG’s using GWO Algorithm,” *IOP Conference Series: Earth and Environmental Science*, vol. 83, no. 1, p. 012003, Jul. 2017.

[2] W. Mohd, Dahalan, and H. Mokhlis, “Network reconfiguration for loss reduction with distributed generations using PSO,” in *Proceedings of 2012 IEEE International Conference on Power and Energy (PECon)*, Kota Kinabalu, Malaysia, Dec. 2012, pp. 823-828.

[3] V. Farahani, B. Vahidi, and H. A. Abyaneh, “Reconfiguration and capacitor placement simultaneously for energy loss reduction based on an improved reconfiguration method,” *IEEE Transactions on Power Systems*, vol. 27, no. 2, pp. 587-595, Feb. 2011.

[4] A. F. Nematollahi, A. Dadkhah, O. A. Gashteroodkhani *et al*., “Optimal sizing and siting of DGs for loss reduction using an iterative-analytical method,” *Journal of Renewable and Sustainable Energy*, vol. 8, no. 5, p. 055301, Sept. 2016.

[5] S. Jazebi, S. H. Hosseinian, and B. Vahidi, “DSTATCOM allocation in distribution networks considering reconfiguration using differential evolution algorithm,” *Energy conversion and Management*, vol. 52, no. 7, pp. 2777-2783, Jul. 2011.

[6] I. Diaaeldin, S. A. Aleem, A. El-Rafei *et al*., “Optimal network reconfiguration in active distribution networks with soft open points and distributed generation,” *Energies*, vol. 12, no. 21, p. 4172, Nov. 2019.

[7] S. Zhang, H. Cheng, D. Wang *et al*., “Distributed generation planning in active distribution network considering demand side management and network reconfiguration,” *Applied Energy*, vol. 228, pp. 1921-1936, Oct. 2018.

[8] Q. Qi, J. Wu, L. Zhang *et al*., “Multi-objective optimization of electrical distribution network operation considering reconfiguration and soft open points,” *Energy Procedia*, vol. 103, pp. 141-146, Dec. 2016.

[9] C. Wang, G. Song, P. Li *et al*., “Optimal siting and sizing of soft open points in active electrical distribution networks,” *Applied Energy*, vol. 189, pp. 301-309, Mar. 2017.

[10] M. R. Dorostkar-Ghamsari, M. Fotuhi-Firuzabad, M. Lehtonen *et al*., “Value of distribution network reconfiguration in presence of renewable energy resources,” *IEEE Transactions on Power Systems*, vol. 31, no. 3, pp. 1879-1888, Aug. 2015.

[11] M. Zarei and A. Zangeneh, “Multi-objective optimization model for distribution network reconfiguration in the presence of distributed generations,” *International Transactions on Electrical Energy Systems*, vol. 27, no. 12, pp. 1-18, Dec. 2017.

[12] W. Cao, J. Wu, N. Jenkins *et al*., “Benefits analysis of soft open points for electrical distribution network operation,” *Applied Energy*, vol. 165, pp. 36-47, Mar. 2016.

[13] Q. Qi and J. Wu, “Increasing distributed generation penetration using network reconfiguration and soft open points,” *Energy Procedia*, vol. 105, pp. 2169-2174, May 2017.

[14] Y. Ahmed, Hatata, and A. Lafi, “Ant lion optimizer for optimal coordination of DOC relays in distribution systems containing DGs,” *IEEE Access*, vol. 6, pp. 72241-72252, Nov. 2018.

[15] M. Norshahrani, H. Mokhlis, A. A. Bakar *et al*., “Progress on protection strategies to mitigate the impact of renewable distributed generation on distribution systems,” *Energies*, vol. 10, no. 11, p. 1864, Nov. 2017.

[16] N. Bayati, A. Dadkhah, S. H. H. Sadeghi *et al*., “Considering variations of network topology in optimal relay coordination using time-current-voltage characteristic,” in *Proceedings of 2017 IEEE International Conference on Environment and Electrical Engineering and 2017*

IEEE Industrial and Commercial Power Systems Europe (EEEIC/ I&CPS Europe), Milan, Italy, Jun. 2017, pp. 1-5.

[17] S. K. Bhattacharya and S. K. Goswami, "Distribution network reconfiguration considering protection coordination constraints," *Electric Power Components and Systems*, vol. 36, no. 11, pp. 1150-1165, Oct. 2008.

[18] B. Khorshid-Ghazani, H. Seyedi, B. Mohammadi-Ivatloo *et al*., "Reconfiguration of distribution networks considering coordination of the protective devices," *IET Generation, Transmission & Distribution*, vol. 11, no. 1, pp. 82-92, Jan. 2017.

[19] H. Zhan, C. Wang, Y. Wang *et al*., "Relay protection coordination integrated optimal placement and sizing of distributed generation sources in distribution networks," *IEEE Transactions on Smart Grid*, vol. 7, no. 1, pp. 55-65, Apr. 2015.

[20] M. Baranski and J. Voss, "Non-intrusive appliance load monitoring based on an optical sensor," in *Proceedings of 2003 IEEE Bologna Power Tech Conference Proceedings*, Bologna, Italy, Jun. 2003, pp. 267-274.

[21] M. N. A. Rahim, H. Mokhlis, A. H. A. Bakar *et al*., "Protection coordination toward optimal network reconfiguration and DG sizing," *IEEE Access*, vol. 7, pp. 163700-163718, Nov. 2019.

[22] V. Fathi, H. Seyedi, and B. M. Ivatloo, "Reconfiguration of distribution systems in the presence of distributed generation considering protective constraints and uncertainties," *International Transactions on Electrical Energy Systems*, vol. 30, no. 5, pp. 1-25, May 2020.

[23] M. B. Shafik, H. Chen, G. I. Rashed *et al*., "Adequate topology for efficient energy resources utilization of active distribution networks equipped with soft open points," *IEEE Access*, vol. 7, pp. 99003-99016, Jul. 2019.

[24] Q. Qi, J. Wu, and C. Long, "Multi-objective operation optimization of an electrical distribution network with soft open point," *Applied Energy*, vol. 208, pp. 734-744, Sept. 2017.

[25] W. Cao, J. Wu, N. Jenkins *et al*., "Operating principle of Soft Open Points for electrical distribution network operation," *Applied Energy*, vol. 164, pp. 245-257, Feb. 2016.

[26] A. Aithal, G. Li, J. Wu *et al*., "Performance of an electrical distribution network with soft open point during a grid side AC fault," *Applied Energy*, vol. 227, pp. 262-272, Oct. 2018.

[27] M. Kezunovic, "Fundamentals of power system protection," *The Electrical Engineering Handbook*, *Academic Press*, pp. 787-803, Jan. 2005.

[28] S. Kawambwa, R. Mwifunyi, D. Mnyanghwalo *et al*., "An improved backward/forward sweep power flow method based on network tree depth for radial distribution systems," *Journal of Electrical Systems and Information Technology,* vol. 8, no. 1, pp. 1-18, Dec. 2021.

[29] S&C Electric Company. (2022, Nov.). TCC fuse. [Online]. Available: https://www. sandc. com /en/products – services/products/positrol-fuse-links/#Product%20Details

[30] R. S. Rao, K. Ravindra, K. Satish *et al*., "Power loss minimization in distribution system using network reconfiguration in the presence of distributed generation," *IEEE Transactions on Power Systems*, vol. 28, no. 1, pp. 317-325, Jan. 2012.

Ali Azizi received the B.S. degree in electrical engineering from Urmia University, Urmia, Iran, in 2018, and the M.S. degree in electrical engineering from Amirkabir University of Technology, Tehran, Iran, in 2022. His main research fields include distribution system analysis, optimization, and loss reduction of distribution systems.

Behrooz Vahidi received the B.S. degree in electrical engineering from the Sharif University of Technology, Tehran, Iran, in 1980, the M.S. degree in electrical engineering from Amirkabir University of Technology, Tehran, Iran, in 1989, and the Ph.D. degree in electrical engineering from the University of Manchester Institute of Science and Technology (UMIST), Manchester, U.K., in 1997. From 1980 to 1986, he worked in the field of high voltage in the industry as a Chief Engineer. Since 1989, he has been with the Department of Electrical Engineering at Amirkabir University of Technology, where he is now a Professor. He has authored and co-authored more than 500 papers and 11 books and book chapters on high-voltage engineering and power systems. His main research fields include high voltage, electrical insulation, power system transient, lightning protection, and pulse power technology.

Amin Foroughi Nematollahi received the M.S. degree in electrical engineering from Amirkabir University of Technology (Tehran Polytechnic), Tehran, Iran, in 2016. He is currently working toward the Ph.D. degree at High Voltage Laboratory, Amirkabir University of Technology. His research interests include distribution network planning, optimization, and power system transient.